Sporadic E tidal variability and characteristics over three mid-latitude Digisonde stations

H. Haralambous[1], C. Oikonomou[1], I. Tsagouri[2], A. Belehaki[2], D. Buresova[3], and Z. Mošna[3]

[1] Frederick Research Center, Nicosia, Cyprus
[2] National Observatory of Athens, Penteli, Athens, Greece
[3] Institute of Atmospheric Physics, Prague, Czech Republic
Email: res.ec@frederick.ac.cy

SCOSTEP 14th Quadrennial Solar-Terrestrial Physics Symposium, Toronto 2018, July 9-13

POSTER: [7] Section 3.2

FREDERICK UNIVERSITY

Introduction

1) The **intermediate descending layers (IDLs)** are defined as weak but long-lived ionization layers which appear to detach from the bottomside of the F region and move downwards to gradually merge with **sporadic E layers** below about 120 km. Therefore IDLs convey metal ions to lower altitudes leading to the intensification of Es layers, which are much stronger in terms of ion density and they also descend in altitude although at slower speeds as compared to the IDLs above.
2) The role of lower Thermosphere tides on Es is fundamental. They provide the convergence vertical wind shears needed for the layers to form and build up, while their downward tidal phase progression causes the layer altitude descend
3) Vertical wind shears in the horizontal neutral wind along with the geomagnetic Lorentz forcing can cause long-living metallic ions in the lower thermosphere to move vertically and converge into plasma layers

Objective

To investigate the seasonal variations of sporadic E (Es) and intermediate descending layers (IDL) generated by vertical wind shears in the horizontal thermospheric winds at different latitudes.

1) Steady-state ion momentum equation

$$0 = e(\mathbf{v}_i \times \mathbf{B} + \mathbf{E}) - M\nu_i(\mathbf{v}_i - \mathbf{V}_n)$$

2) Vector components (south, east, up)

$$\mathbf{v}_i = (u, v, w); \quad \mathbf{V}_n = (U, V, W); \quad \mathbf{B} = -B_0(\cos I, 0, \sin I)$$

3) Ion vertical speed for E = 0

$$w = \frac{U \cos I \sin I}{1 + (\nu_i/\Omega_i)^2} + \frac{(\nu_i/\Omega_i) V \cos I}{1 + (\nu_i/\Omega_i)^2}$$

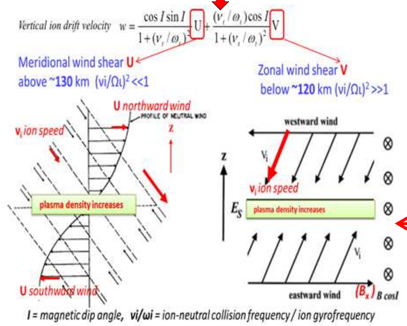

Figure 2. Wind shear mechanism which operates at E and lower F-regions. Meridional (left) and zonal (right) wind shear mechanisms for vertical ion convergence into a thin ionization layer developing at the wind shear velocity null (Haldoupis, 2012).

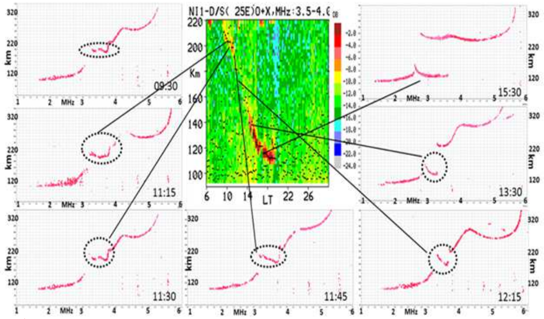

Figure 1. Ionogram HTI plot, computed over a 24 h local day (24 Feb. 2009) in 3.5-4 MHz frequency band. Ionograms corresponding to certain times of HTI plot recorded between 9:30 to 15:30 LT at Nicosia station are also presented. IDL traces are denoted with black dotted circles.

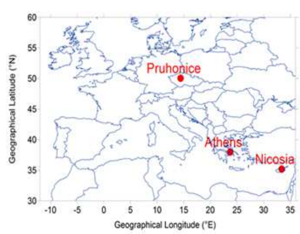

Figure 3. Map showing location of the three mid-latitude ionospheric stations involved in the study.

Data & Methodology

- We used ionograms obtained as shown at Table 1, for an 8- and 5-year period from two Digisondes (DPS-4D) located near Nicosia (35°N, 33°E), Cyprus and Athens (38°N, 23.5°E), Greece respectively, as well as for a 3-year period a Digisonde (DPS-4D) located in Pruhonice (50°N, 14.6°E), Czech Republic. The Digisonde DPS-4D is an advanced ionospheric sounder which conducts optimal ionogram recordings by using the Precision Group Height Measurement (PGHM) technique (Reinisch et al., 2008). Ionograms were recorded every 15, 5 and 15 minutes for Nicosia, Athens and Pruhonice Digisonde respectively.
- The available recordings were analyzed by means of using the 'height-time-intensity' (HTI) method introduced by Haldoupis et al. (2007), which is capable of identifying tidal-like variations in sporadic E and IDL layers. This technique combines individual ionograms, to represent a snapshot of the reflected signal intensity as a function of (virtual) height and ionosonde frequency, and focuses on the ionogram part within a fixed frequency bin. This is repeated on sequential ionograms so that a height-time-intensity plot is obtained for a given frequency bin, in the same way a radar operating at a fixed frequency obtains a range-time-intensity (RTI) plot.

Table 1. List of ionospheric stations, their location and data used in this study

Ionospheric station	Lat (°N)	Lon (°E)	Geomagnetic Lat (°N)	Inclination (dip angle) (°)	Data availability (Years)
Nicosia (Cyprus)	35	33	31.72	52	2009-2016
Athens (Greece)	38	23.5	36.16	54	2009, 2010, 2011, 2015, 2016
Pruhonice (Czech Republic)	50	14.6	49.29	66	2009, 2015, 2016

References

Reinisch, B. W., Galkin, I. A., Khmyrov, G. M., Kozlov, A. V., Lisysyan, I. A., Bibl, K., Cheney, G., Kitrosser, D., Stelmash, S., Roche, K., Luo, Y., Paznukhov, V. V., & Hamel, R. (2008), Advancing Digisonde technology: the DPS-4D, In radio sounding and plasma physics. In: AIP Conference Proceedings, (vol.974, pp.127–143), doi:10.1063/1.2885023.
Haldoupis, C., (2012). Midlatitude sporadic E. A typical paradigm of atmosphere– ionosphere coupling. Space Science Reviews, 168, 441–461.

Acknowledgements

We are highly grateful of Prof. Christos Haldoupis and Dr. Chis Meek for their valuable advice and large contribution on this study. This work was conducted in the frame of Short Term Scientific Mission within the COST Action CA15211 in collaboration with the Institute for Astronomy, Astrophysics, Space Applications and Remote Sensing (IAASARS) of the National Observatory of Athens (NOAA). We also note the support of the SCOSTEP organising committee.

Results

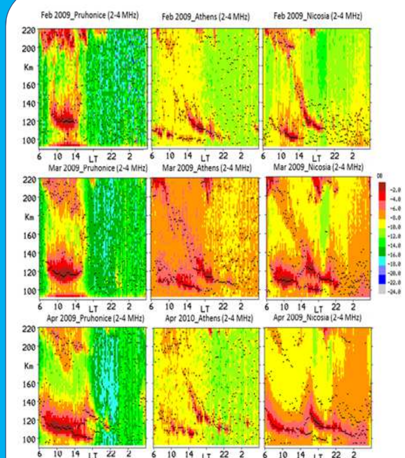

Figure 4. Representative monthly average HTI plots in Pruhonice (left panels), Athens (middle panels) and Nicosia (right panels) for February (up row), March (middle row) and April (down row) respectively. The frequency band used for each plot is also denoted.

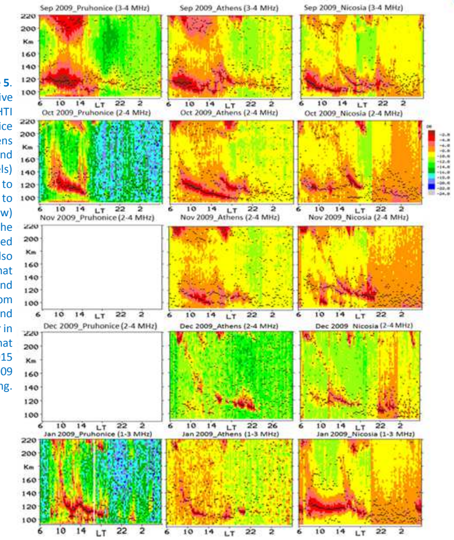

Figure 5. Representative monthly average HTI plots in Pruhonice (left panels), Athens (middle panels) and Nicosia (right panels) for September to January (from up to down row) respectively. The frequency band used for each plot is also denoted. Note that all plots correspond to 2009, except from November and December in Pruhonice that corresponds to 2015 as data for 2009 were missing.

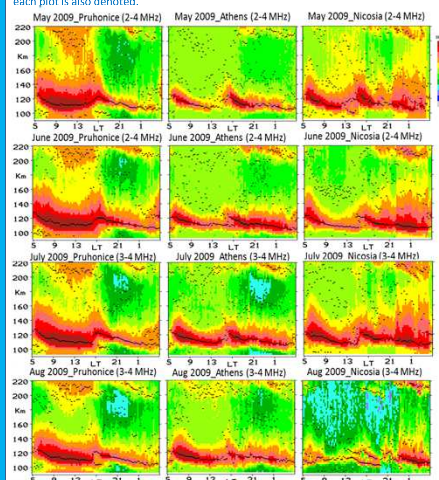

Figure 6. Representative monthly average HTI plots in Pruhonice (left panels), Athens (middle panels) and Nicosia (right panels) for May to August 2009 (from up to down row) respectively. The frequency band used for each plot is also denoted.

Conclusions

- The HTI traces of Es and IDL layers observed in all three locations are characterized mostly by a 12-hour periodicity in layer occurrence and descent, albeit some differences that exist in layer occurrence and intensity.
- For the first time, additional shorter-scale periodicities in IDL and Es occurrence are detected. Specifically, a 6-hour periodicity is observed during winter in all stations and around equinoxes only in Pruhonice. An 8-hour periodicity is also found mainly in the lower mid-latitude stations during summer. These periodicities can be attributed to the semi-, quarter- and terd- diurnal thermospheric tides respectively.
- Our results confirmed that: (a) the semidiurnal tides are dominant at mid-latitudes during the whole year and (b) the terdiurnal tides become active during summertime at lower and occasionally at higher mid-latitudes. The quarter-diurnal tides though weaker than semidiurnal ones, are consistent through all years and can also affect the formation of ionization layers primarily in higher and less in lower mid-latitude regions.
- For the first time evidence of a 4-hour periodicity only in January in Pruhonice is provided, possibly due to the interaction between tides and atmospheric gravity waves.

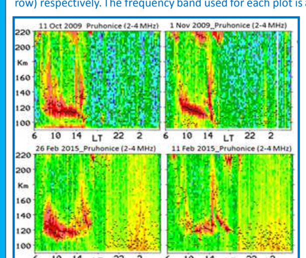

Figure 7. Characteristic daily HTI plots near spring and autumn equinoxes in Pruhonice in 2009 (upper panels) and 2015 (low panels) where a 6-hour periodicity in Es and IDL reflection traces is prevailing.

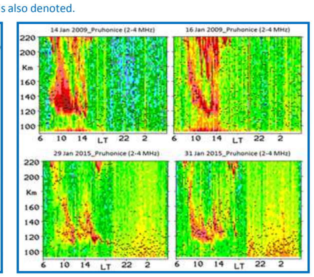

Figure 8. Characteristic daily HTI plots during January 2009 and 2015 in Pruhonice where a 4-hour periodicity is present.

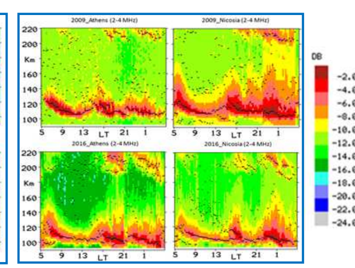

Figure 9. Average HTI plots showing a terdiurnal (8h) periodicity of sporadic E layer occurrence and altitude descent in Athens and Nicosia stations around summer solstice 2009 (upper panels) and 2016 (lower panels).